



FIRST SOLPS-ITER WIDE GRID SIMULATIONS OF THE ITER BURNING PLASMA SCRAPE-OFF LAYER

E. KAVEEVA, N. SHTYRKHUNOV, V. ROZHANZKY, I. SENICHENKOV Peter the Great St. Petersburg Polytechnic University, St. Petersburg, Russian Federation

Email: E.Kaveeva@spbstu.ru

R.A. PITTS, X. BONNIN, A. PSHENOV ITER Organization, St Paul Lez Durance Cedex, France

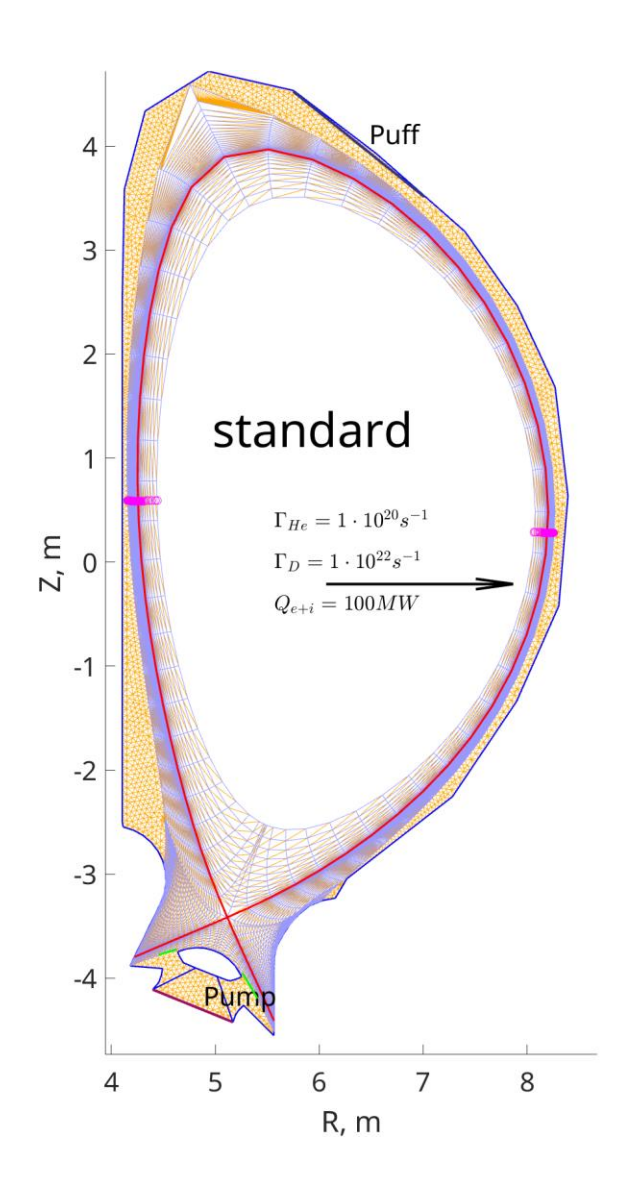
OUTLINE

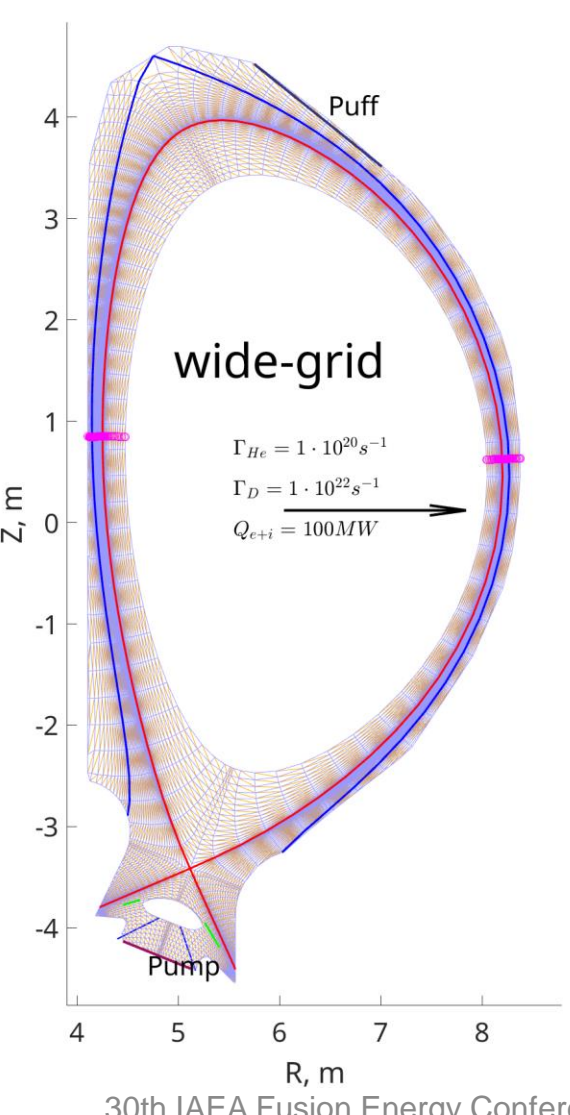
- Motivation
- Grid modifications
- Benchmarking to standard grid results in near SOL
- Increased SOL transport: choice of transport parameters
- Modeling setup and 2D plots
- OMP profiles for various transport in far SOL
- Targets profiles for various transport in far SOL
- Main chamber wall flows
- Conclusions

Motivation

- ITER re-baseline assumes full W wall of main chamber
- Contamination of plasma by W sputtered from the wall can be an issue
- Nowadays tokamaks show a "shoulder" formation of high density in OMP far SOL in the semi-detached/pronounced detachment regimes, increasing wall sputtering
- The flows in far SOL and W migration description in future reactors demands the modeling up to the wall of machine
- Standard SOLPS-ITER 3.0.9 mesh spans only up to the artificial "last flux surface in SOL"
- The modeling extension up to the wall is necessary

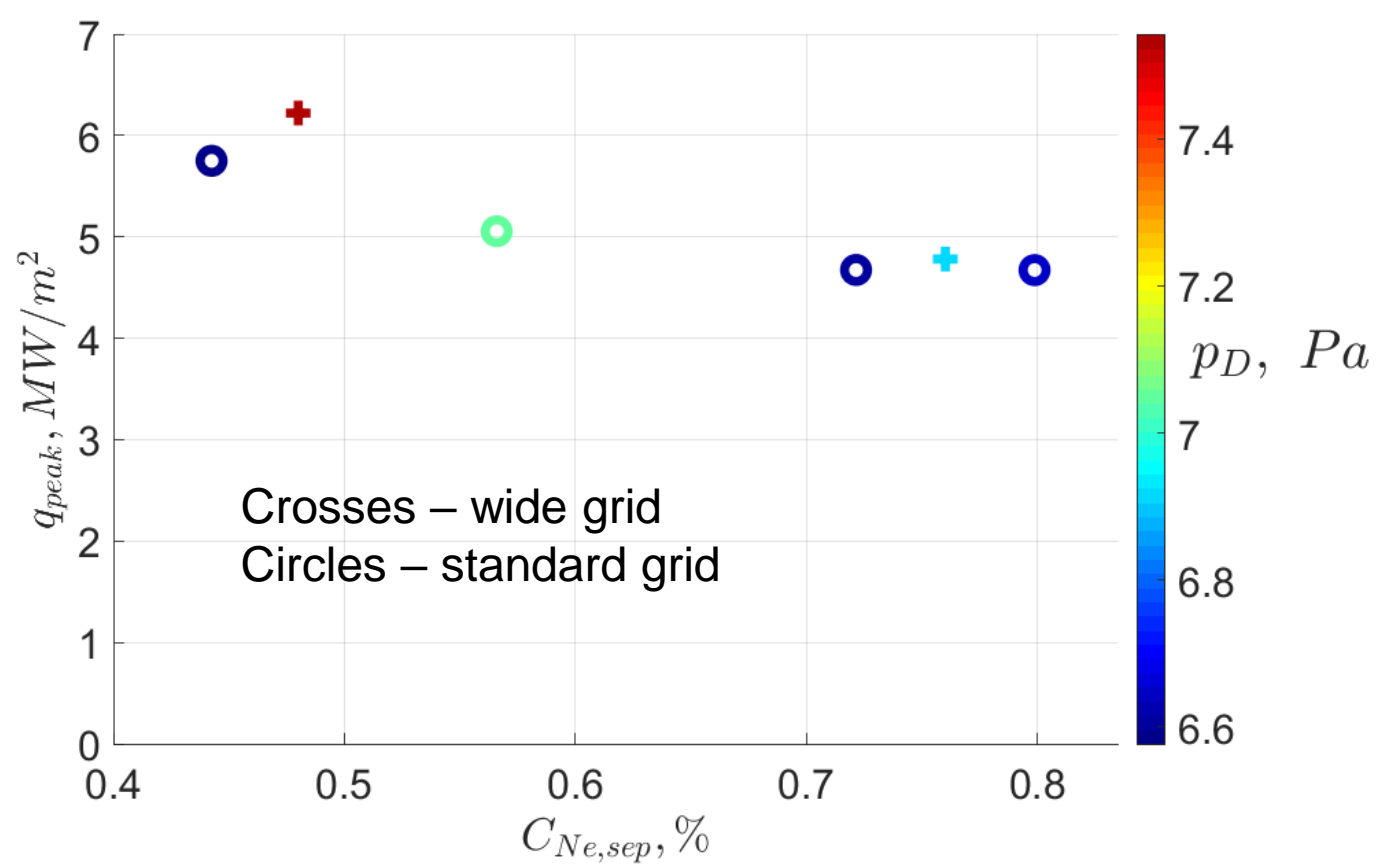
New code SOLPS-ITER 3.2.0. Grid modifications





- Now plasma grid covers all the chamber, together with EIRENE grid
- Some flux tubes start and finish on the main chamber wall or under the dome
- Secondary X-point just on the wall is possible
- Necessary data rearrangement: unstructured grid

Benchmarking to standard grid results in near SOL



Outer target heat load (here and further on: toroidally symmetric, without account of W monoblock shaping) as a function of Ne concentration at the separatrix.

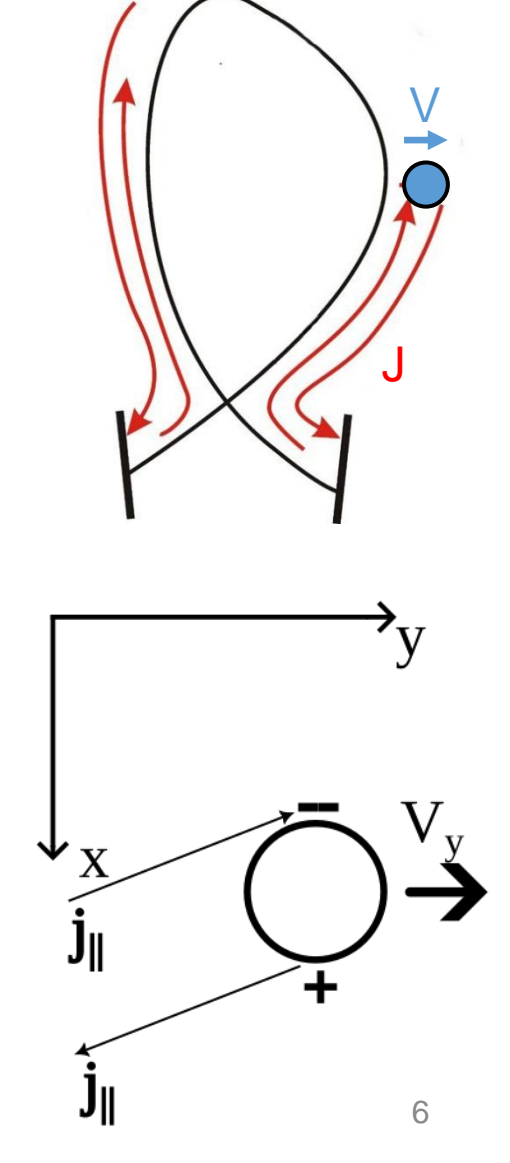
On the wide grid the target load is bigger, but still of the same order

- $D_{AN,farSOL} = 0.3 \, m^2/s$
- Puffing of deuterium $5 \cdot 10^{22} s^{-1}$
- Neon seeding is varied from $6.75 \cdot 10^{19} s^{-1}$ to $12 \cdot 10^{19} s^{-1}$ for standard grid and from $4.5 \cdot 10^{19} s^{-1}$ to $9 \cdot 10^{19} s^{-1}$ for wide grid case.
- Pumping coefficient set by feedback scheme to achieve deuterium atoms and molecules pressure in the PFR $P_D = 7Pa$.
- Wall contour shot IMAS #116000, run#4.
- $P_{e+i} = 100MW$.
- $B_t = 5.3T$, $I_p = 15MA$
- Full EIRENE description
- With SOL potential and thermoelectric current
- But no drifts

Choice of transport parameters in far SOL: simple estimate

Assumption:

- transport by filaments in a range of some typical most stable dimensions which follow each after the other, without big time delay
- closing of ∇B driven currents through targets
- typical filament radial propagation length of the same order as its initial size.



Choice of transport parameters in far SOL: simple estimate

Estimate for diffusion coefficient

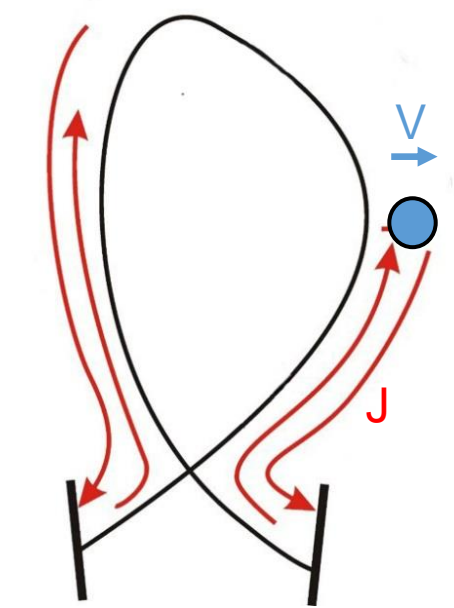
$$D = \left(\frac{T_e}{e}\right)^{4/3} B^{-4/3} \left(1 + \frac{T_i}{T_e}\right)^{2/3} \left(\frac{4r}{R^2 b_x c_s}\right)^{1/3} \left(\frac{R_{vol} + R_{sh}}{R_{shomp}}\right)^{2/3}$$

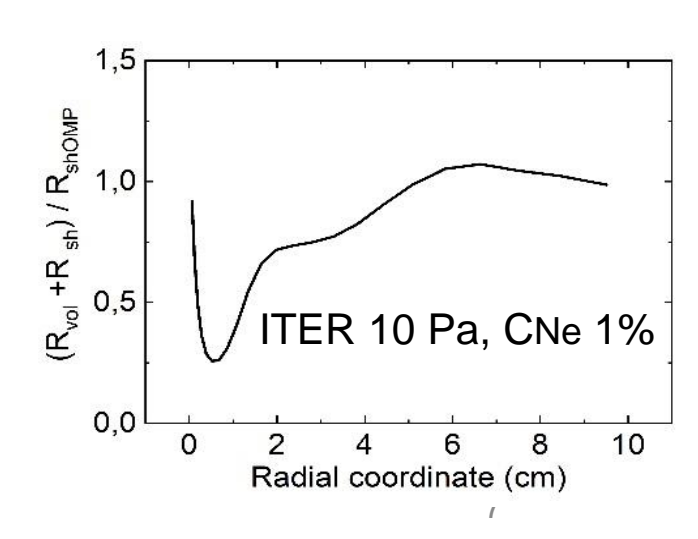
 R_{vol} , R_{sh} - effective resistivity of volume and sheath

 Parameters for estimate are taken from SOLPS-ITER modeling of ITER full burning plasma, and of ASDEX-Upgrade experiment

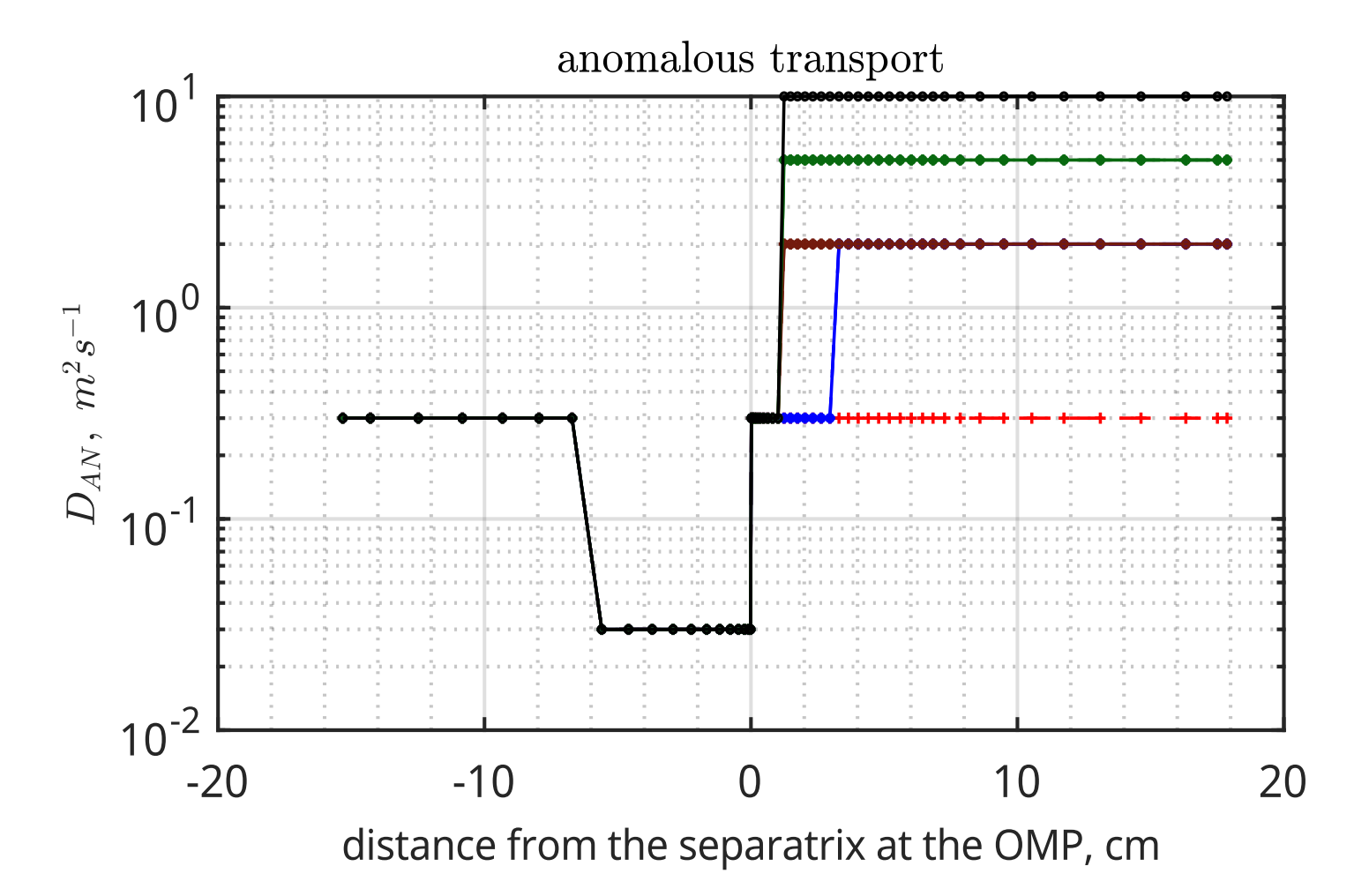
Results

- ASDEX-Upgrade: $D = 2.2m^2/s$
- ITER: $D = 2 m^2/s$



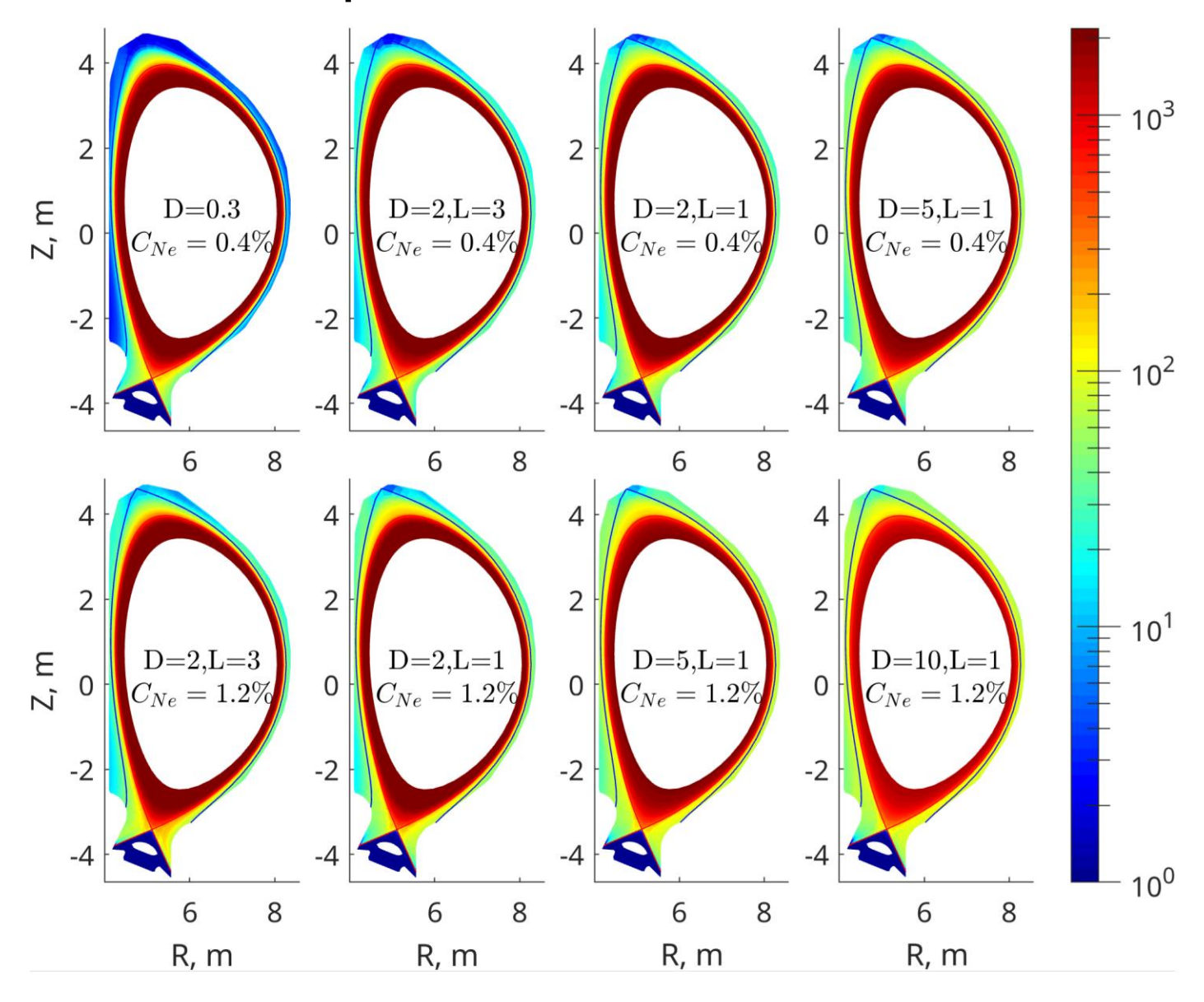


Choice of SOL transport parameters: modeling



- The parameters were varied in a wide range to cover uncertainties in the transport estimate
- $D = 0.3 10 \, m^2/s$
- Lowest transport corresponds to modeling database for standard grid
- Two choices for distance where the transport is increased: 1 or 3 cm from separatrix
- Ratio $\chi_{i,e}/D_{AN}$ =3.3 kept the same as in the database for standard grid

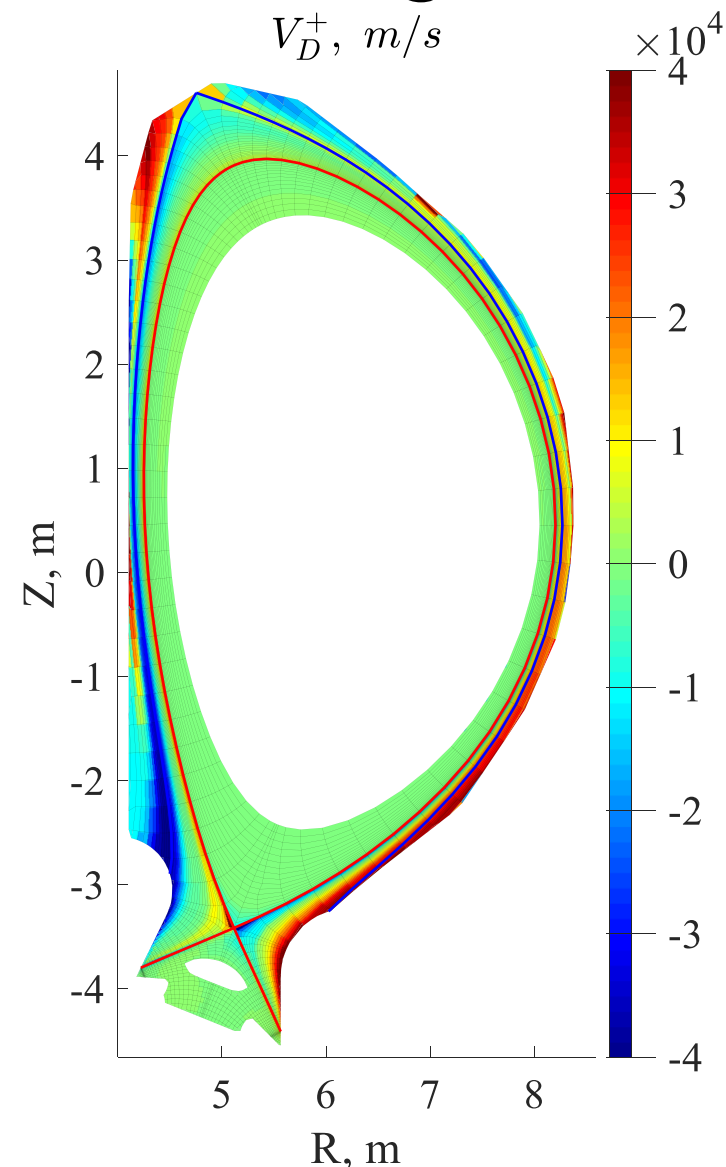
Ions temperature eV



Modeling setup

- Puffing of deuterium $5 \cdot 10^{22} s^{-1}$
- Neon separatrix concentration set by seeding feedback $C_{Ne}=0.4\%$ or $C_{Ne}=1.2\%$.
- Pumping coefficient feedback to achieve D atoms and molecules pressure in the PFR $P_D = 7Pa$.
- Wall contour shot IMAS #116000, run#4.
- $P_{e+i} = 100MW$
- $B_t = 5.3T$, $I_p = 15MA$
- Full EIRENE description
- With SOL potential and thermoelectric current
- But no drifts

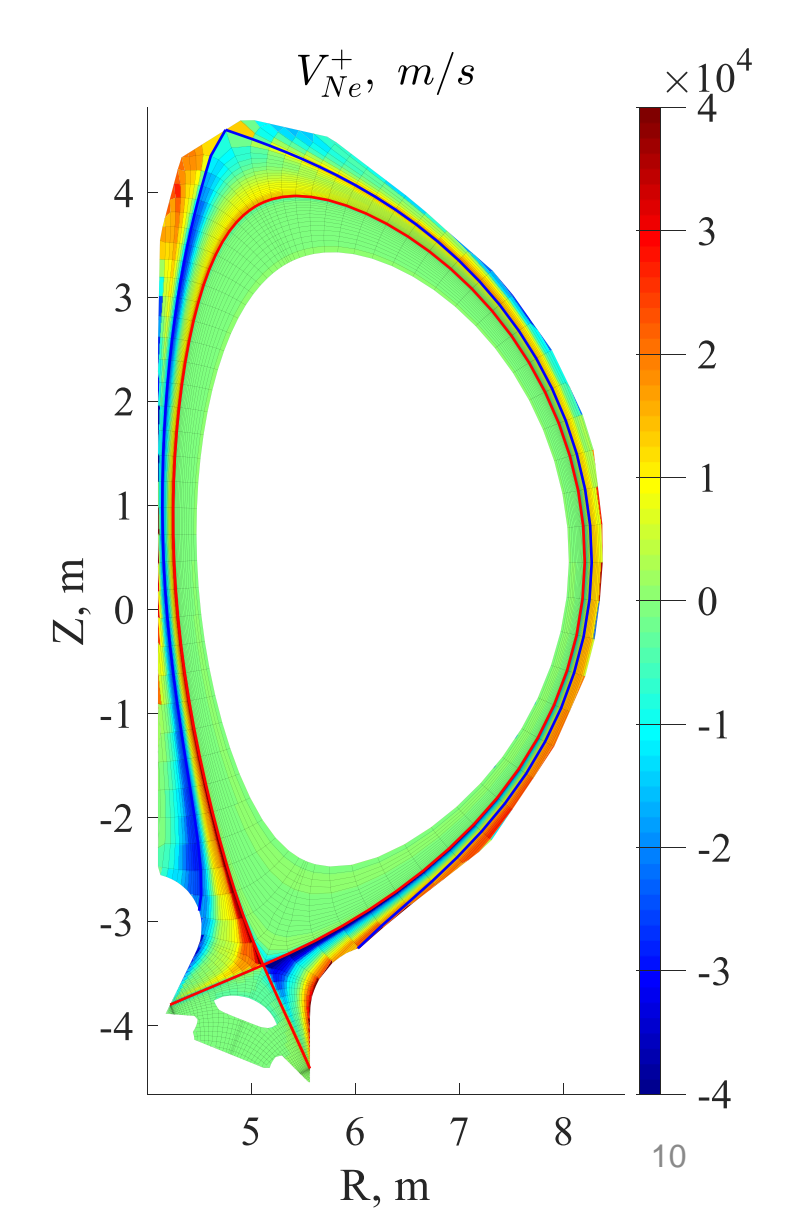
Parallel velocity "background" for W migration modeling

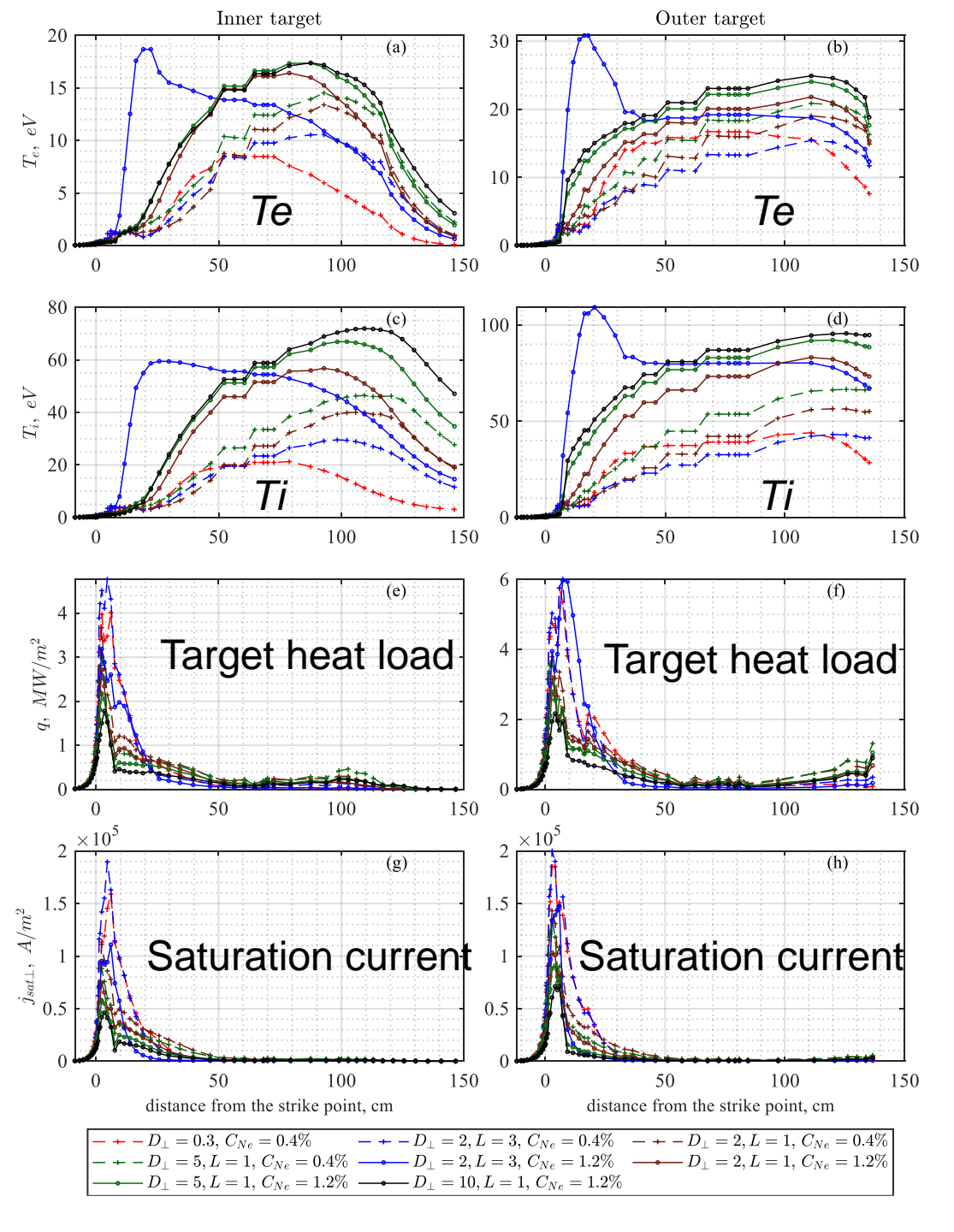


- The parallel velocity for all species is calculated up to the main chamber wall
- Boundary condition of sound-speed flow towards the wall is applied almost everywhere at the main chamber wall

Plots for $D = 2 m^2/s$ in far SOL

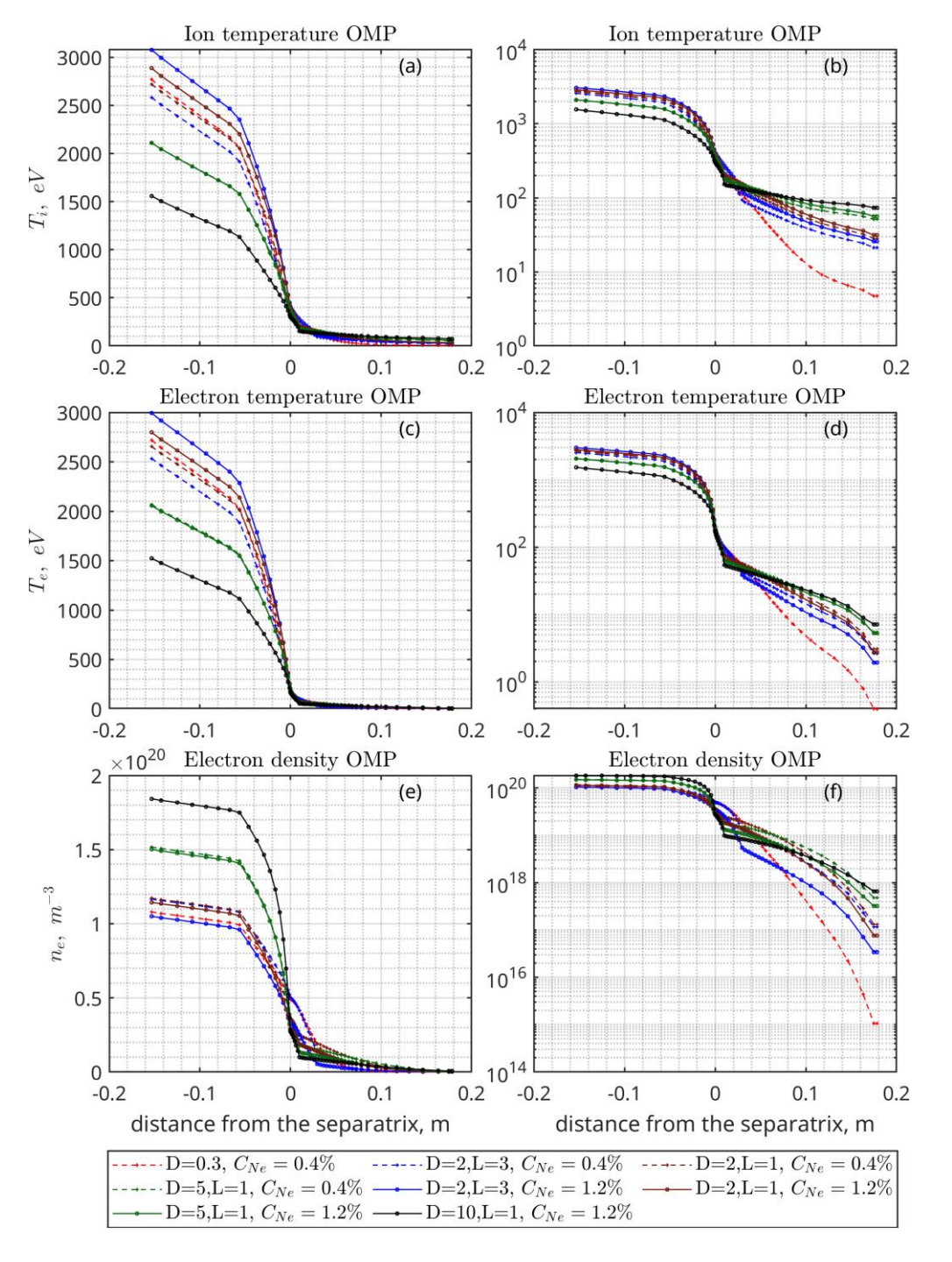
30th IAEA Fusion Energy Conference 13–18 October 2025, Chengdu, China





Target profiles

- All the regimes are semi-detached (temperature at the strike point < 5 eV)
- Target heat load decreases with the far SOL radial transport increase; in all the regimes it is acceptable
- The ions temperature in far SOL increases with transport increase



Outer midplane profiles characteristic lengths in far SOL

$$\lambda_{T_e}/\lambda_n > 1, \qquad \lambda_{T_i}/\lambda_n > 1$$

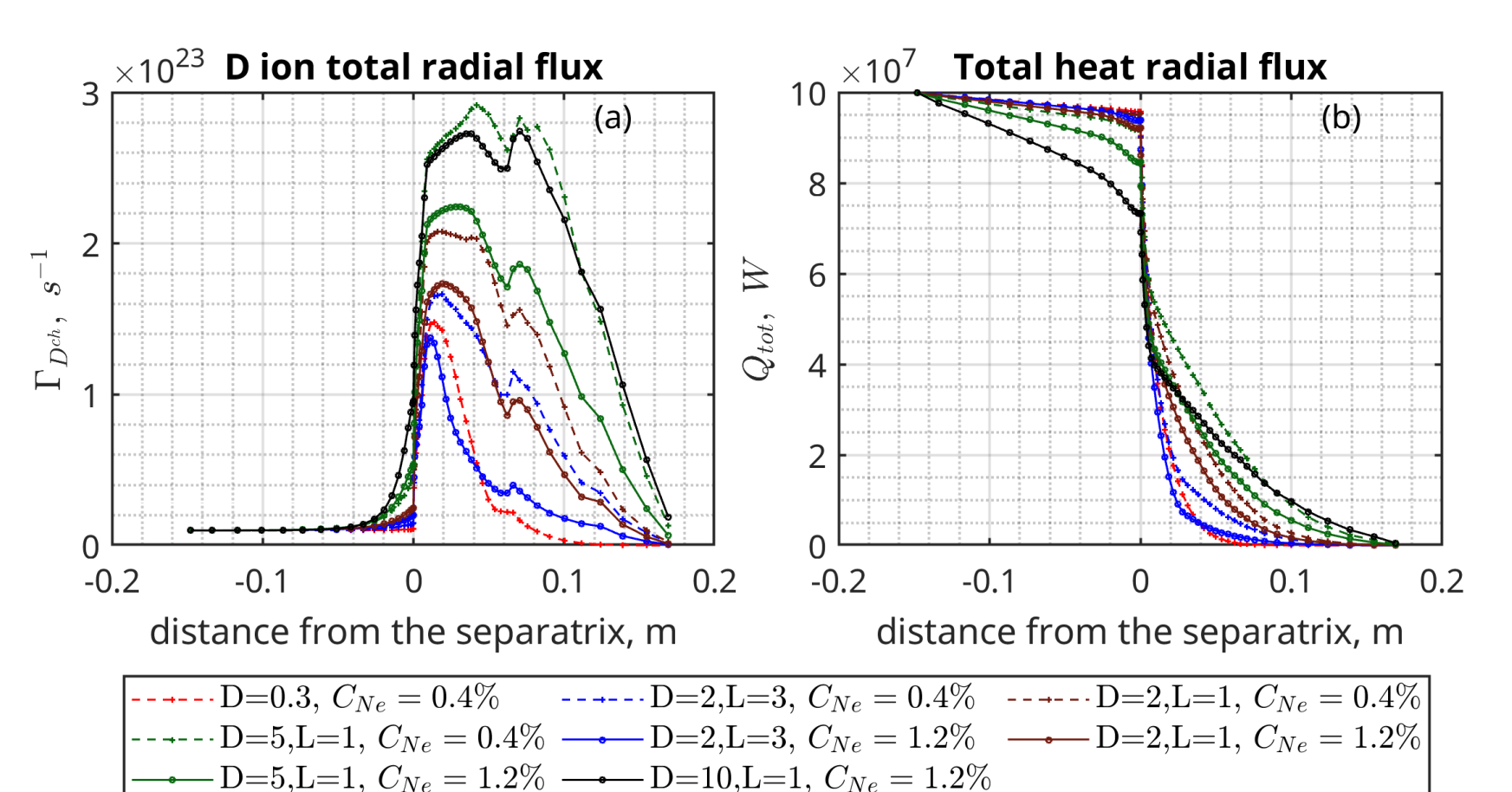
Can be explained by simple balance

$$\nabla \cdot \left(\frac{3}{2}nT_{e,i}(\vec{V}_{diff} + \vec{V}_{||}) + \vec{q}\right) = -nT_{e,i}\nabla \cdot \vec{V}_{||}$$

with account of corresponding sheath transmission factors

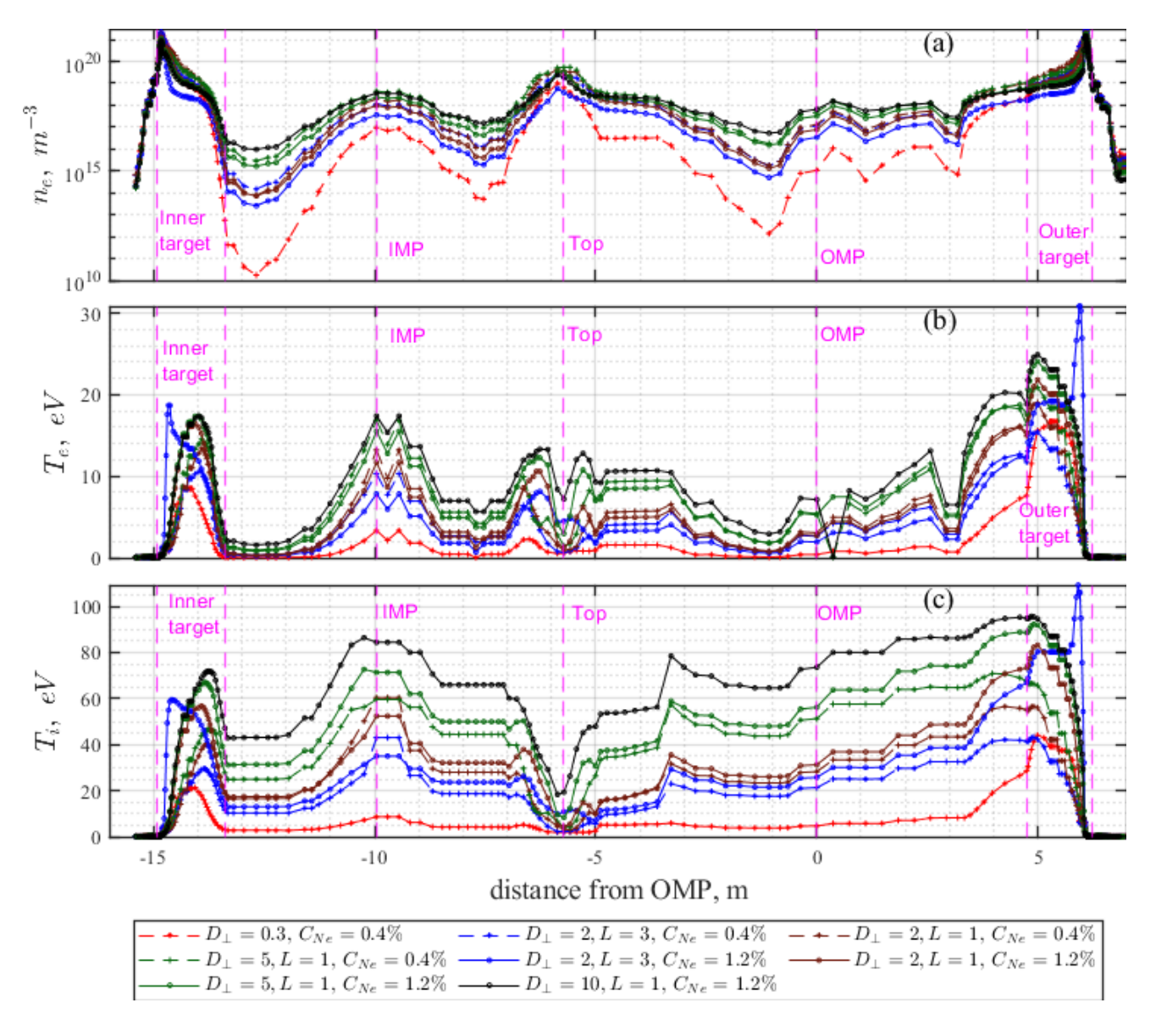
| Label | C _{Ne} , % | $\lambda_{T_{ ho}}$, cm | λ_{T_i} , cm | λ_n , cm | λ_{T_e}/λ_n | λ_{T_i}/λ_n |
|----------|---------------------|--------------------------|----------------------|------------------|---------------------------|---------------------------|
| D=0.3 | 0.4 | 3.7 | 7.8 | 1.7 | 2.2 | 4.7 |
| D=2,L=3 | 0.4 | 5.3 | 13.1 | 2.9 | 1.8 | 4.5 |
| D=2,L=1 | 0.4 | 5 | 12.5 | 2.7 | 1.8 | 4.6 |
| D=5,L=1 | 0.4 | 5.8 | 22.5 | 3.6 | 1.6 | 6.2 |
| D=2,L=3 | 1.2 | 5.2 | 12.9 | 2.9 | 1.8 | 4.5 |
| D=2,L=1 | 1.2 | 5 | 12.2 | 2.7 | 1.8 | 4.5 |
| D=5,L=1 | 1.2 | 6.1 | 20.4 | 3.6 | 1.7 | 5.7 |
| D=10,L=1 | 1.2 | 6.8 | 35.3 | 4.8 | 1.4 | 7.4 |

Radial flows in the main chamber



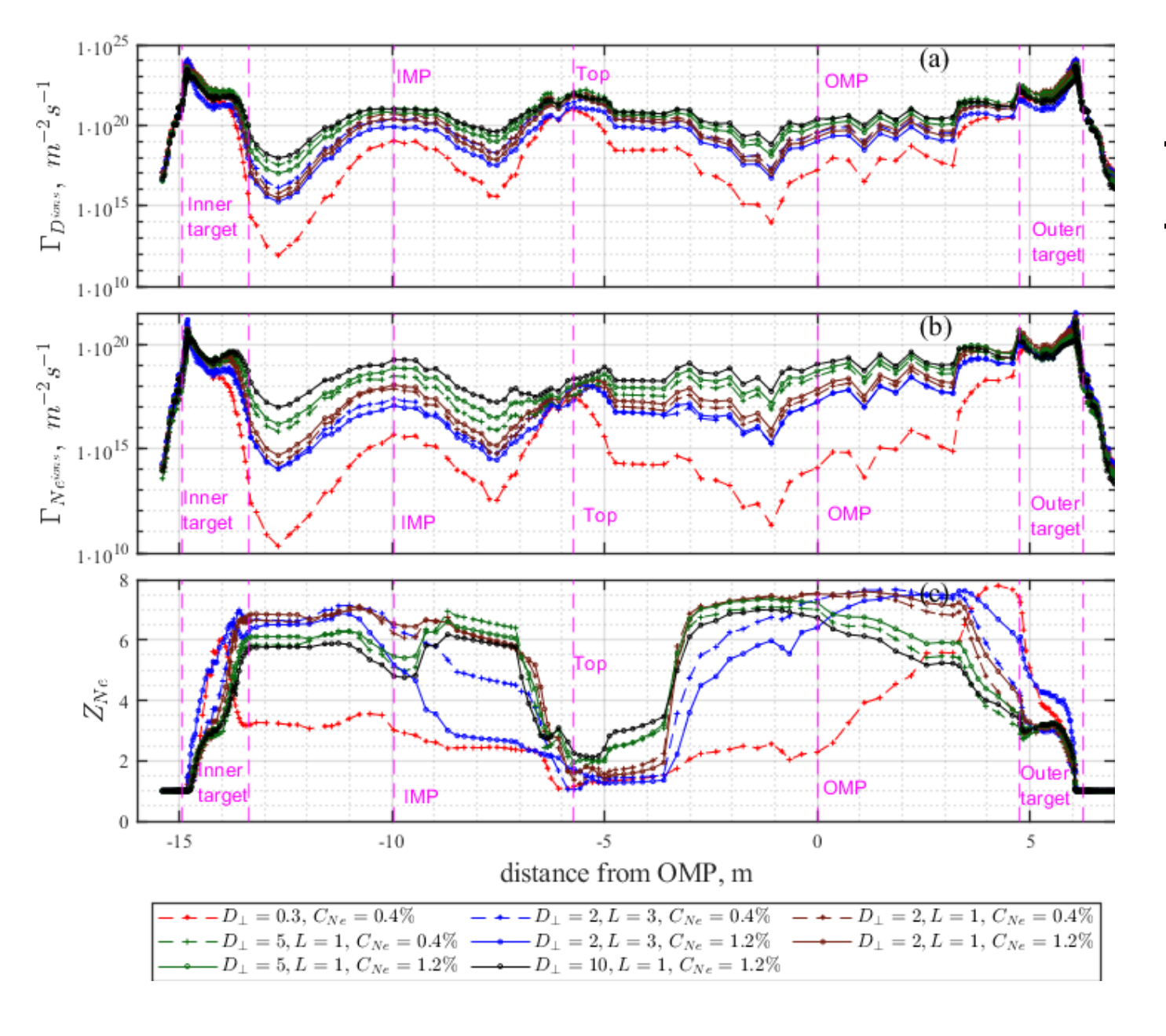
With transport coefficients increase:

- Radial flows towards the wall increase
- Ionization and the heat losses inside the separatrix increase



Distribution of density and temperature at the main chamber wall

- Noticeable rise of temperatures at inner midplane and at the outer divertor entrance.
- Temperatures drop and electron density peak at the top of the first wall corresponding to the secondary Xpoint position.
- Significant temperatures increase in case of big radial transport
- Ions temperature is big due to its small radial decay length



Distribution of plasma flows and Ne charge at the main chamber wall

- Both main ions and radiating impurity flows increase by orders of magnitude in case of density shoulder formation.
- Neon charge(on average) Z = 6 can be expected

Conclusions

- The modeling of burning plasma edge for ITER with the new SOLPS-ITER 3.2.0 code version in the geometry extended to the main chamber wall is performed for the first time.
- Primary aim of the numerical study was realistic description of the plasma flows onto the wall, and simulation of plasma background for the study of tungsten sputtering and migration by other codes.
- The SOLPS-ITER 3.2.0 results were compared with SOLPS-ITER 3.0.8 modeling ones on the standard narrower grid. The comparison was done for constant moderate SOL transport, previously typically used for ITER modeling with SOLPS-ITER 3.0.7-3.0.9. In the common computational domain the codes give close results.
- The transport coefficients in the far SOL were increased in a wide range up to factor 30, in order to simulate the possible widening of SOL, so-called shoulder formation. As a result, in the limiting case the density characteristic scale in the far SOL has increased approximately by factor of 3.
- The flow of main ions and seeded impurity to the wall at the outer and inner midplanes increases by approximately two orders of magnitude when the diffusion coefficient increases from $D_{AN,farSOL} = 0.3 \, m^2/s$ to $D_{AN,farSOL} = 2 \, m^2/s$. The last value can be taken as reasonably pessimistic scenario.
- The temperatures decay lengths in the far SOL are bigger than that for density. The electron temperature decreases at the scales comparable to that of density, while the ion temperature decreases considerably slower. The ions temperature decay length can exceed ten centimeters, leading to high (of the order of several tens of eV) ion temperature at the wall.

BACKUP slides

Simple model for far SOL characteristic length

$$\frac{d}{dy}D\frac{dn}{dy} = \frac{n}{\tau}$$

$$\tau = \frac{L}{b_x c_s}.$$

$$n = n \Big|_{y=0} exp(-y/\lambda_n)$$

$$\lambda_n = \sqrt{D\tau} = \sqrt{DL/b_x c_s}.$$

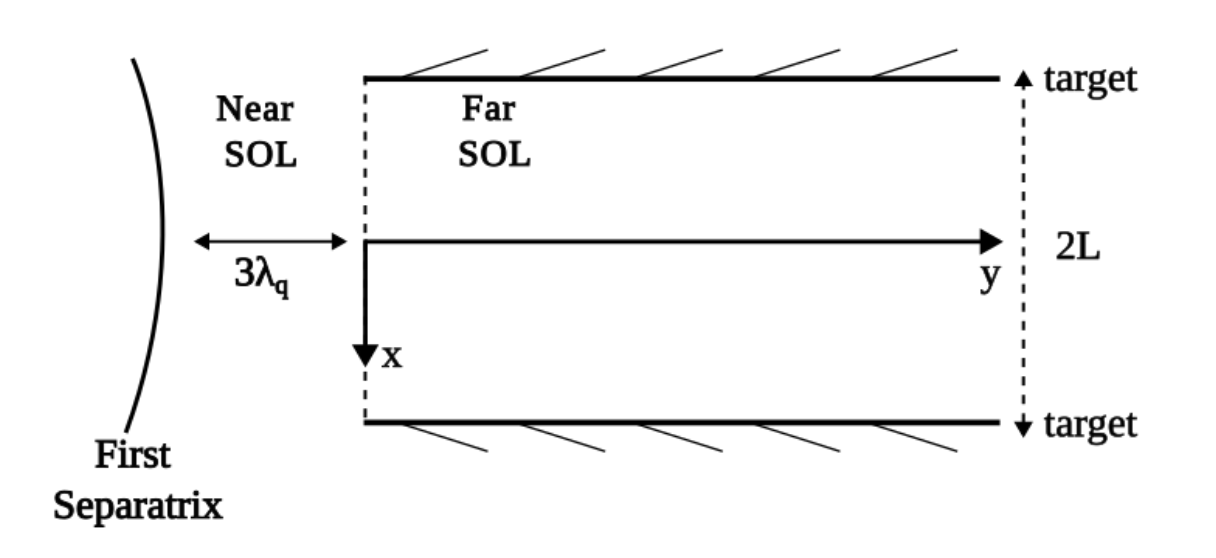
$$\nabla \cdot \left(\frac{5}{2}nT_i\vec{V}_{||} + \frac{3}{2}nT_i\vec{V}_y + \vec{q}\right) = \vec{V}_{||} \cdot \nabla nT_i$$

$$\frac{3}{2}V_{y}\frac{\partial nT_{i}}{\partial y} + \frac{3}{2}V_{x}\frac{\partial nT_{i}}{\partial x} + \frac{3}{2}nT_{i}\frac{\partial V_{y}}{\partial y} + \frac{5}{2}nT_{i}\frac{\partial V_{x}}{\partial x} = -\frac{\partial q_{x}}{\partial x} - \frac{\partial q_{y}}{\partial y}$$

$$q_{x} = -b_{x}^{2}\chi_{i\parallel}n\partial T_{i}/\partial x \qquad q_{y} = -n\chi_{i\perp}\partial T_{i}/\partial y$$

$$\gamma_i n T_i b_x c_s = \frac{5}{2} n T_i V_x(L) + q_x(L)$$

$$T_{i} = T_{i}(0) \exp(-y/\lambda_{T_{i}}) \qquad \Longrightarrow \qquad \left(\gamma_{i} - \frac{3}{2}\right) \left(\frac{\lambda_{T_{i}}}{\lambda_{n}}\right)^{2} - \left(\frac{3}{2} + \frac{\chi_{i\perp}}{D}\right) \frac{\lambda_{T_{i}}}{\lambda_{n}} - \frac{\chi_{i\perp}}{D} = 0$$



$$\frac{3}{2}\frac{DL}{\lambda_n}\frac{\partial nT_i}{\partial y} + \frac{5}{2}nT_iV_x(L) = -q_x(L) + L\frac{\partial}{\partial y}\left(n\chi_{i\perp}\frac{\partial T_i}{\partial y}\right)$$

Model for diffusion coefficient

Model for the diffusion in sheath limited regime

$$j_{||} = I_g/l_{\perp} = \frac{2\delta n(T_e + T_i)l_{||}}{BRl_{\perp}}$$

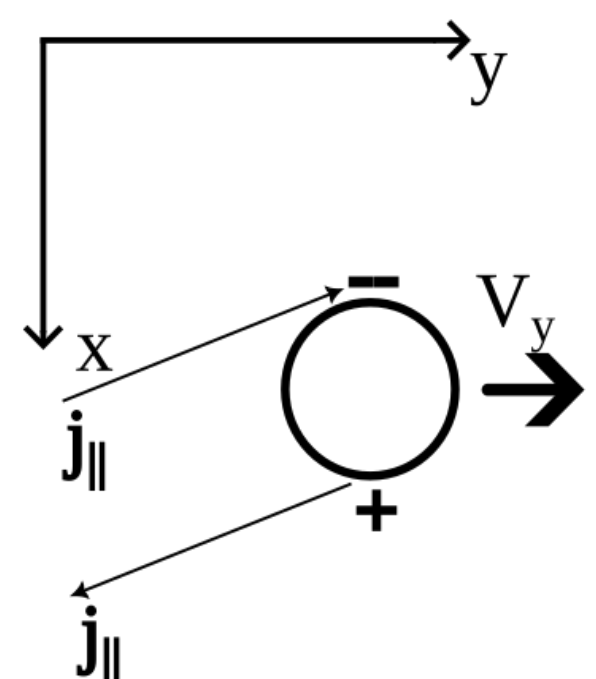
$$j_{||} = enc_s \frac{e\delta \varphi}{T_e}$$

$$\delta \varphi = \frac{2\delta n(T_e + T_i)T_el_{||}}{nc_s e^2 BRl_{\perp}} \longrightarrow V_y = \frac{2\delta n(T_e + T_i)T_el_{||}}{nc_s e^2 B^2 Rl_{\perp}^2}$$

$$\delta n = l_{\perp} \frac{\partial n}{\partial r} = l_{\perp} \frac{n}{\lambda_n}$$
 $\langle \delta n V_y \rangle = \frac{2n(T_e + T_i)T_e l_{||}}{c_s e^2 B^2 R \lambda_n^2}$

$$\langle \delta n V_y \rangle / \lambda_n \approx n c_s / l_{||} \longrightarrow \lambda_n \approx \left(\frac{2(T_e + T_i) T_e l_{||}^2}{e^2 B^2 R c_s^2} \right)^{1/3}$$

$$D n/\lambda_n^2 \approx n c_s/l_{||}$$
 \longrightarrow $D \approx \left(\frac{2(T_e + T_i)T_e}{e^2 B^2}\right)^{2/3} \left(\frac{q}{c_s R}\right)^{1/3}$



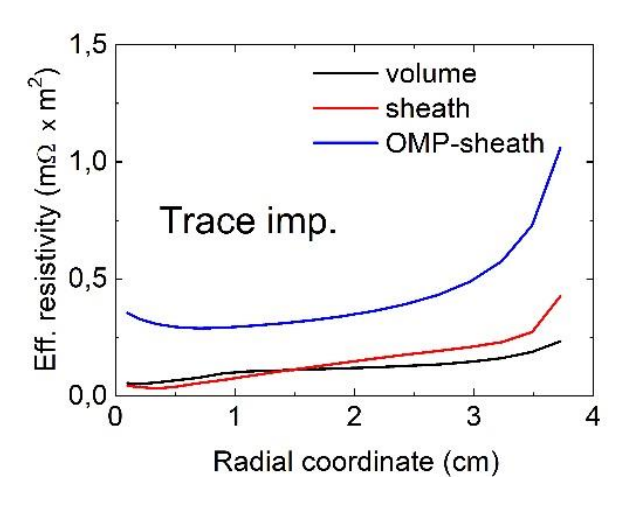
Model for the diffusion in conduction limited regime

$$\delta\varphi = \frac{2\delta n(T_e + T_i)T_e l_{||}}{nc_s e^2 BR l_{\perp}} \qquad \Longrightarrow \qquad \delta\varphi = \frac{2\delta n(T_e + T_i)T_e l_{||}}{nc_s e^2 BR l_{\perp}} \frac{R_{vol} + R_{sh}}{R_{shoMP}}$$

$$D \approx \left(\frac{2(T_e + T_i)T_e}{e^2B^2}\right)^{2/3} \left(\frac{q}{c_sR}\right)^{1/3} \qquad \longrightarrow \qquad D \approx \left(\frac{2(T_e + T_i)T_e}{e^2B^2} \frac{R_{vol} + R_{sh}}{R_{shomp}}\right)^{2/3} \left(\frac{q}{c_sR}\right)^{1/3}$$

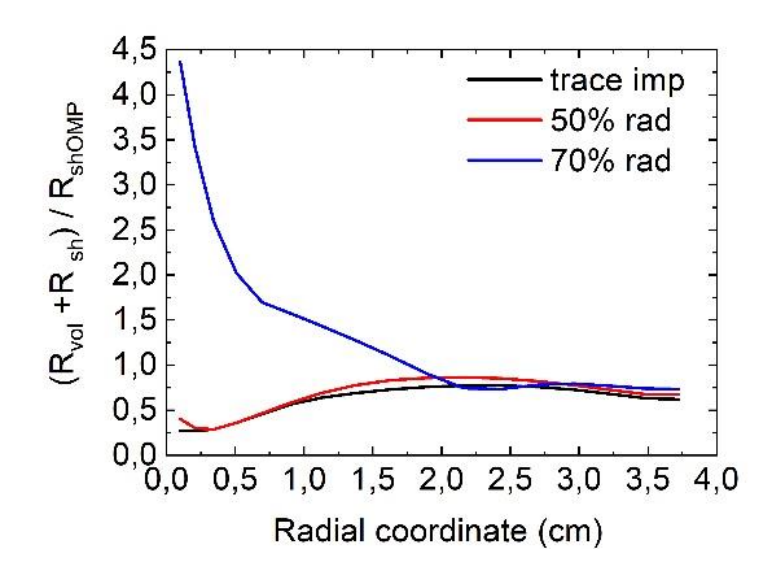
It is seen in modeling that the ratio $\frac{R_{vol}+R_{sh}}{R_{shoMP}}$ is the same in semi-detached regimes of ASDEX-Upgrade and ITER

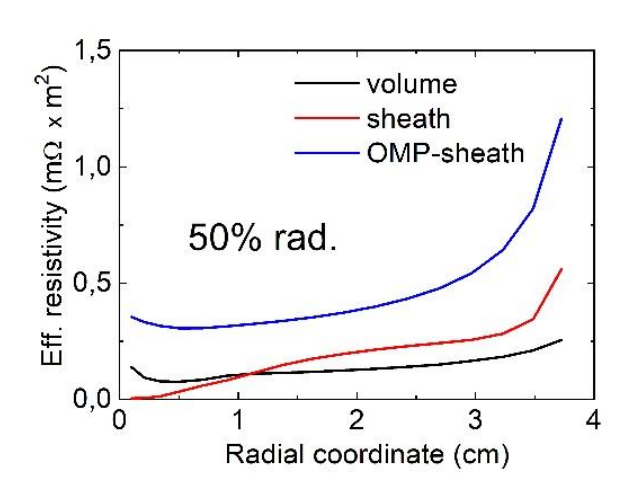
Resistivity of SOL and sheath in ASDEX Upgrade modeling



$$T_{e \ sep} = 119eV$$

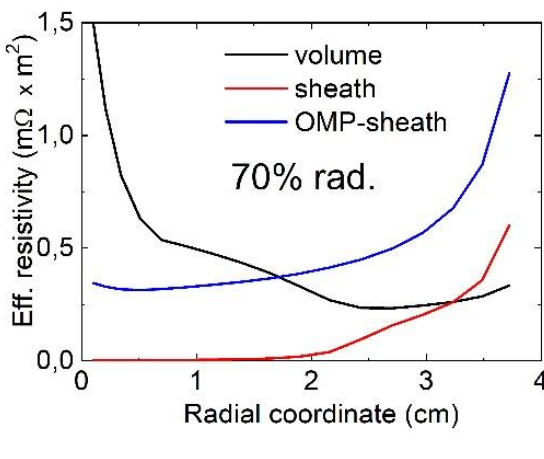
$$T_{e\ t(\text{max})} = 23eV$$





$$T_{e \ sep} = 114eV$$

$$T_{e\ t(\text{max})} = 16eV$$



$$T_{e \ sep} = 101eV$$

$$T_{e\ t(\text{max})} = 6eV$$

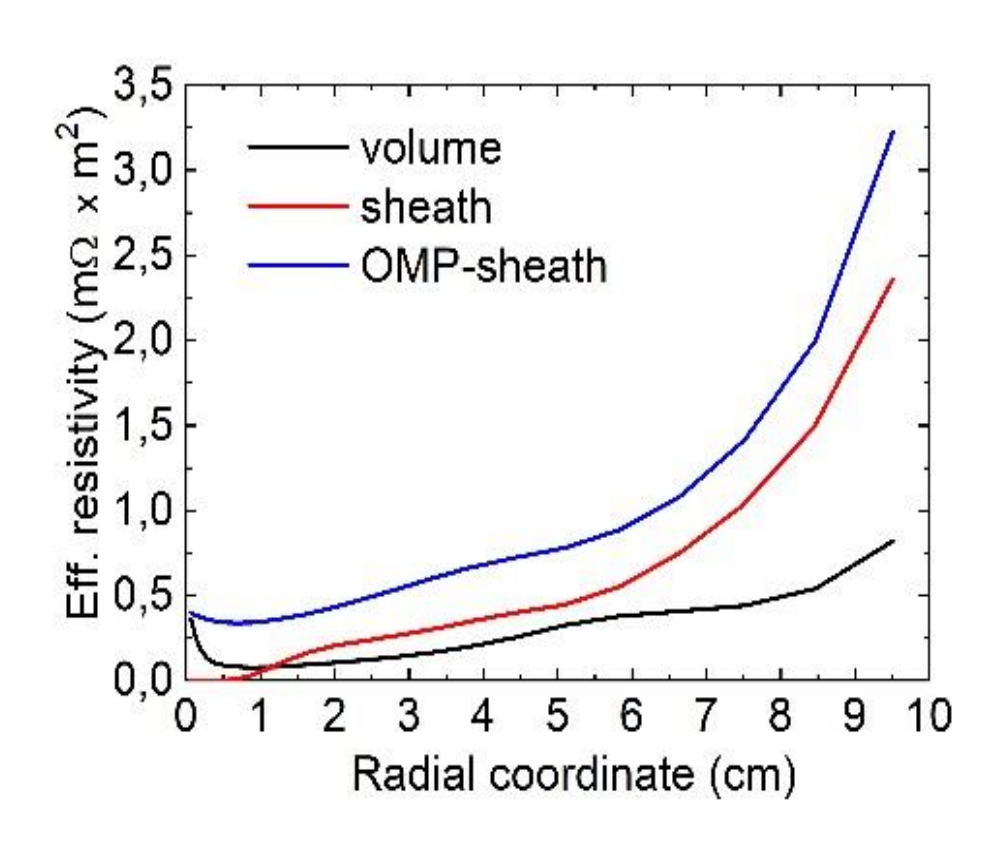
$$n_{e \ sep} = 3.1 - 3.3 \cdot 10^{19} m^{-3}$$

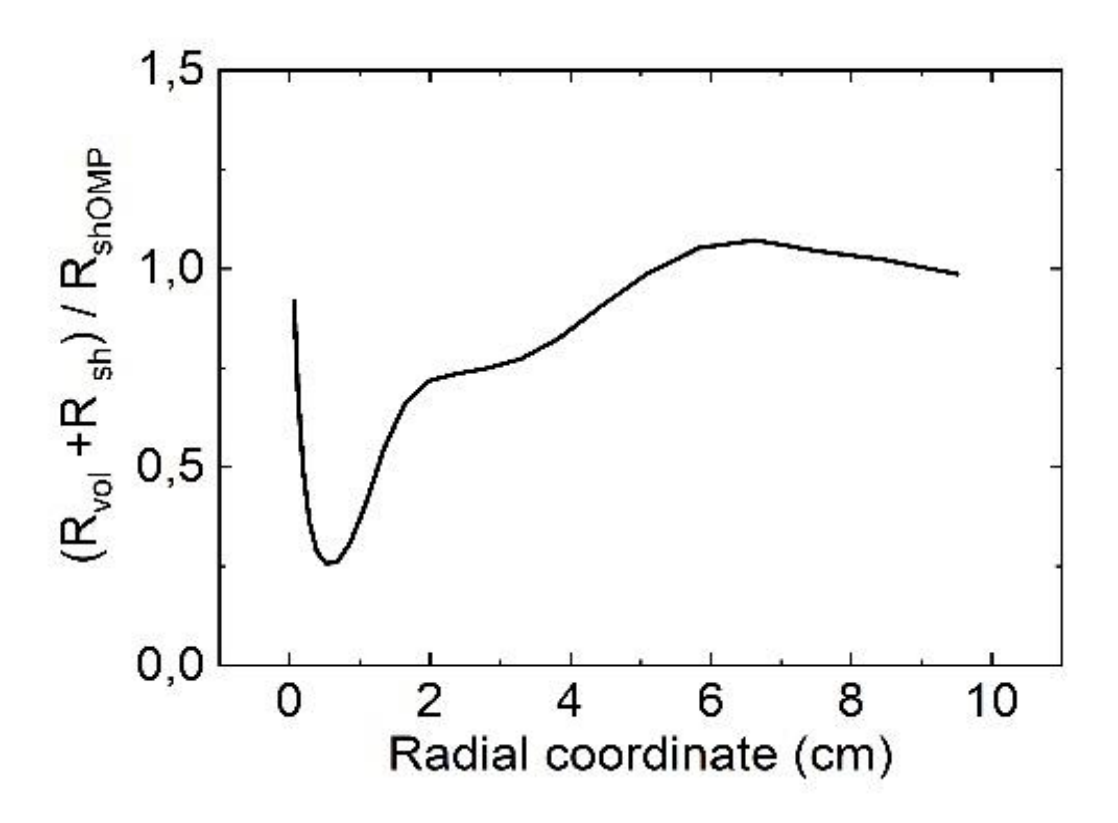
Resistivity significantly differs from the estimate based on OMP parameters only for pronounced detachment

$$R_{vol} = \frac{\varphi_{OMP} - \varphi_{Sh}}{j_{||OMP}} = \frac{1}{B_{OMP}} \int_{OMP}^{t} \frac{Bh_x dx}{\sigma_{||} b_x}$$

$$R_{sh} = \frac{\varphi_{sh}}{j_{||OMP}} = \frac{B_t}{B_{OMP}} \frac{T_{et}}{e^2 n_t c_{s_t}}$$

Resistivity of SOL and sheath in ITER modeling





Estimates / parameters

For the semi-detached ASDEX-Upgrade case with 50% radiation the assumption $\frac{R_{vol} + R_{sh}}{R_{shomp}} = 1$ remains valid.

The diffusion coefficient may be estimated from Eq.(33) taking the SOL parameters at the OMP.

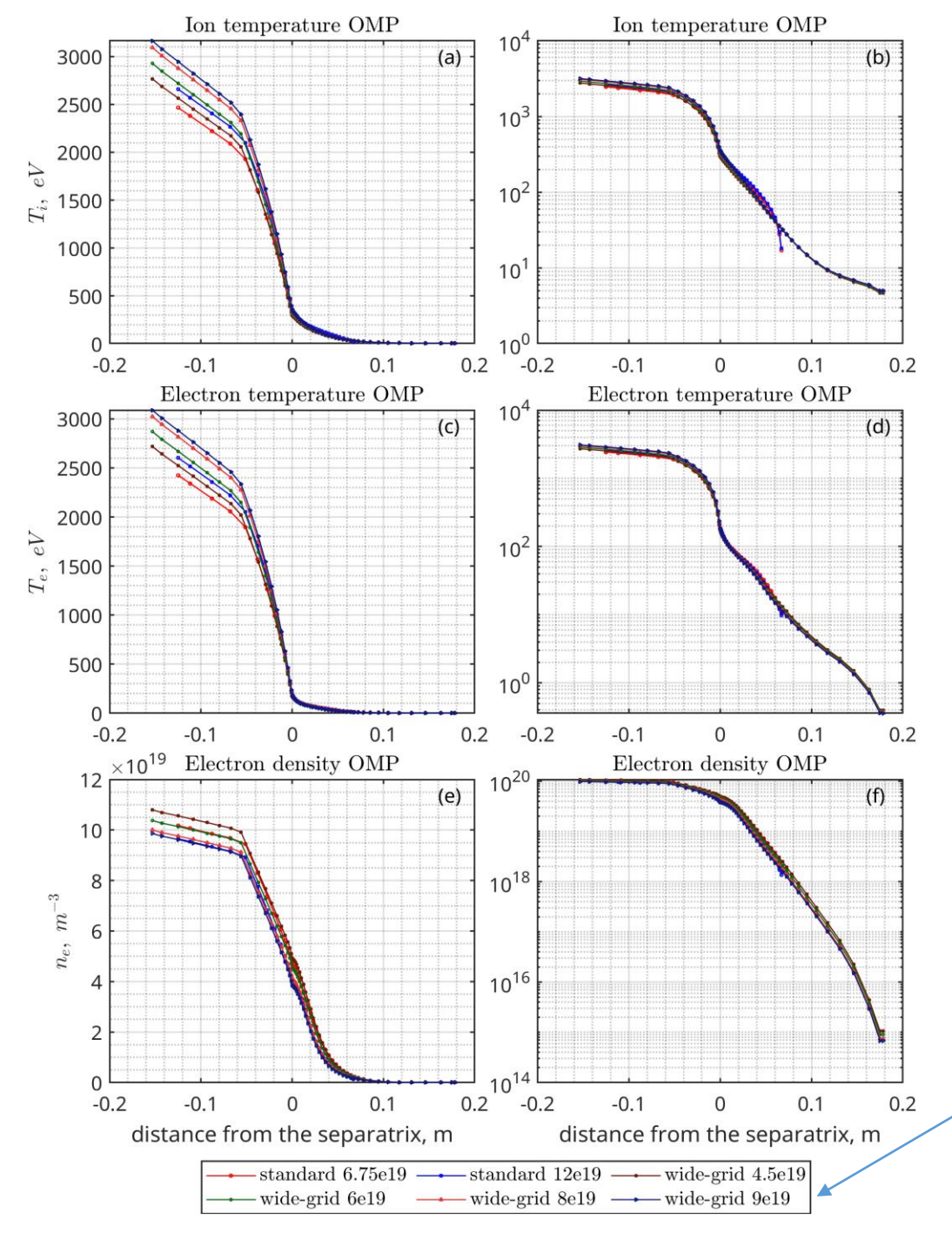
Choosing
$$\frac{T_e}{e} = 20 \text{ eV}$$
, $B = 2T$, $\frac{T_i}{T_e} = 2$, $b_x = 0.1$, $R = 1.75 \text{ m}$, $r = 0.5 \text{ m}$, a diffusion coefficient $D = 2.2m^2/s$ is obtained.

According to the authors' experience from fitting experimental ASDEX Upgrade SOL profiles during the SOLPS-ITER modelling exercise, this estimated effective diffusion coefficient is in reasonable agreement with the values typically required in such modelling ($D = 1.5 \, m^2/s$ [36]).

For ITER H-modes, the SOL T_e and toroidal magnetic field will be around a factor of 2 higher than in ASDEX Upgrade. This would yield a diffusivity of $D = 2.0m^2/s$ and therefore very similar to that in ASDEX Upgrade in the region with dominating filamentary transport mechanism.

$$D \approx \left(\frac{2(T_e + T_i)T_e}{e^2 B^2} \frac{R_{vol} + R_{sh}}{R_{shomp}}\right)^{2/3} \left(\frac{q}{c_s R}\right)^{1/3}$$

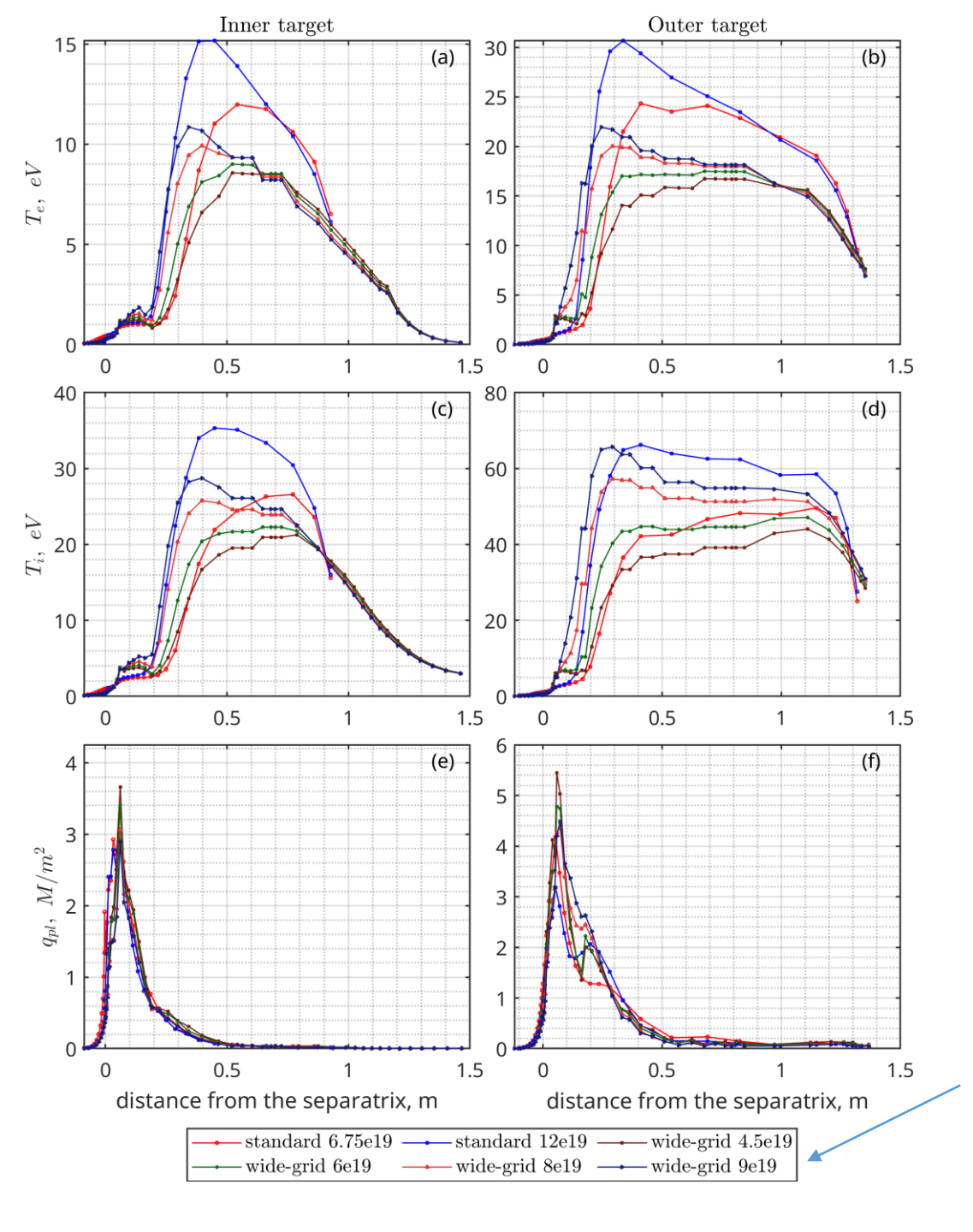
Benchmarking to standard grid results



Benchmarking to standard grid results in near SOL: OMP

 Parameters are close to each other for the low far SOL transport

Numbers give seeding values to produce different Ne concentrations at the separatrix



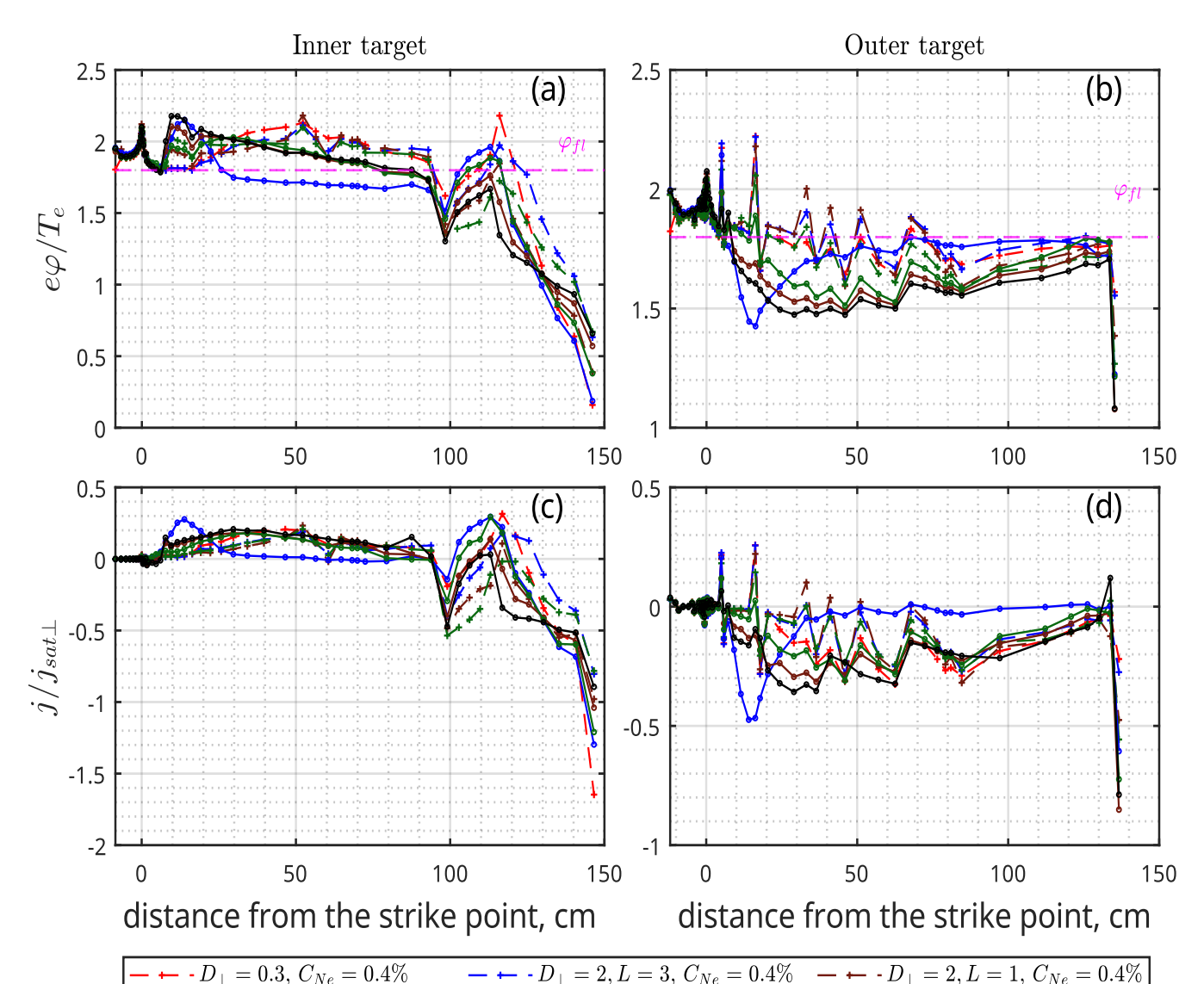
Benchmarking to standard grid results in near SOL: targets

 Parameters are close to each other for the low far SOL transport

Numbers give seeding values to produce different Ne concentrations at the separatrix

Role of currents in SOL

Potential and current on the inner and outer divertor targets



 $-D_{\perp} = 2, L = 1, C_{Ne} = 1.2\%$ \longrightarrow $D_{\perp} = 10, L = 1, C_{Ne} = 1.2\%$

- Profiles of $e\varphi/T_e$ (floating potential 1.80 T_e/e , corresponding to $\delta_e=0.5$ is defined by magenta line). This parameter can affect the acceleration of ions at the target and as a consequence the target sputtering.
- $\mathrm{j}/j_{j_{sat\perp}}$ ratio of the electric current at the target to the ion saturation current, indicating considerable difference between the ion and electron flows to the target. The electron flow enters the energy flow to the target, as well as the electrostatic potential. Positive direction of current is from the inner and towards the outer target.

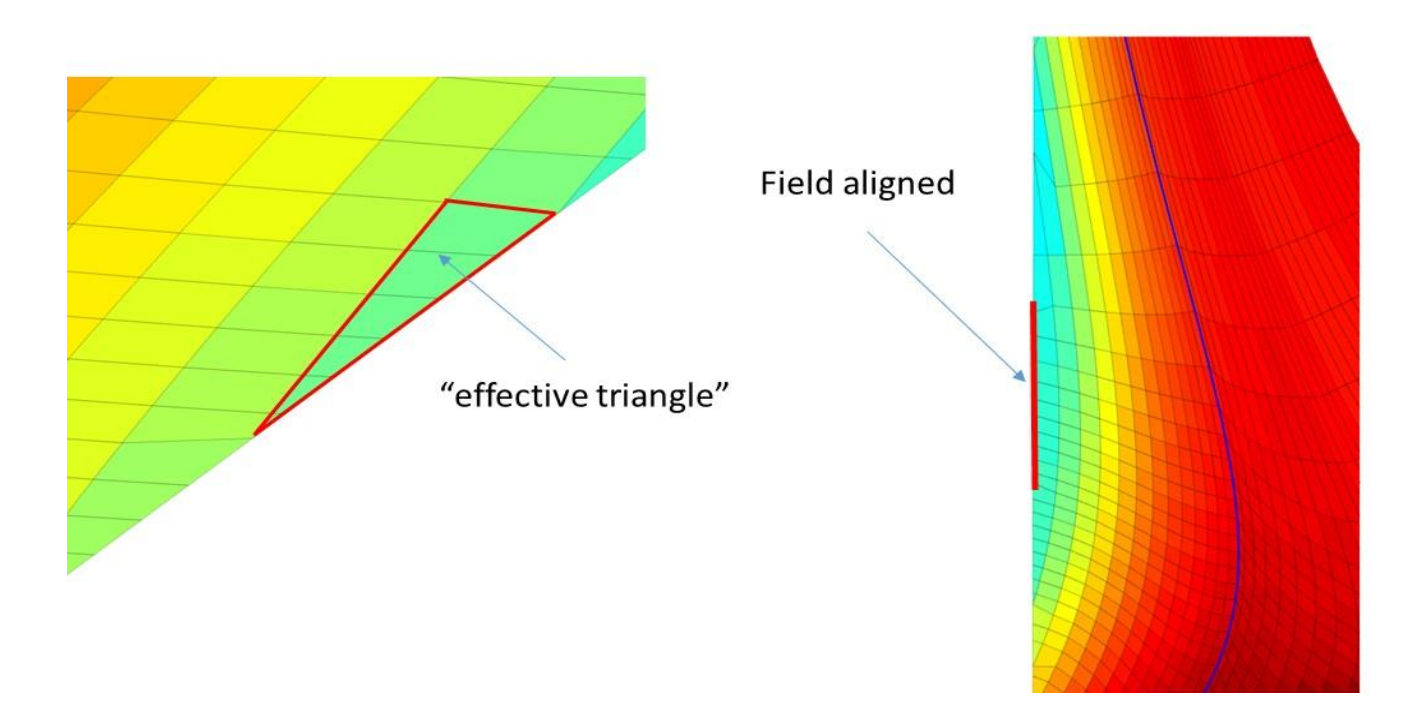
For the modeling without current balance, the floating electrostatic potential is assumed, while the electron flow is taken equal to the ion flow, which influences the heat flow calculation.

 $- \leftarrow -D_{\perp} = 5, L = 1, C_{Ne} = 0.4\%$ \longrightarrow $D_{\perp} = 2, L = 3, C_{Ne} = 1.2\%$ \longrightarrow $D_{\perp} = 5, L = 1, C_{Ne} = 1.2\%$ ≥ 13–18 October 2025,

Numerical and physical issues in far SOL wide grid modeling

Boundary conditions:

- separation of field aligned and non-field aligned boundaries
- treatment of non-field aligned sequence of trapezoidal and triangular cell faces at the ends of flux tubes



Flux limiting and heat sources in low $\int_{wall_1}^{wall_2} v_{ii} \frac{dl}{c_s} \le 1$ collisionality far-SOL regions

$$\int_{wall1}^{wall2} v_{ii} \frac{dl}{c_s} \le 1$$

For the flux tube length comparable to the ions mean free path:

$$\tilde{k}_{||i} \approx k_{||i} \frac{1}{1 + \frac{k_{||i}b_{\theta}^{2}|\nabla_{\theta}T_{i}|}{c_{f \lim_{1}}b_{\theta}T_{i}}}$$

$$\frac{1}{1 + \left(c_{f \lim_{2}}\int_{wall_{1}}^{wall_{2}}v_{ii}\frac{dl}{c_{s}}\right)^{-1}}$$

No heat sources:
$$Q^{vis} = \sum_{a=0}^{n_s-1} \left(\eta_{a||} b_{\theta}^2 (\nabla V_{a||})_{\theta}^2 + \eta_{ANa} (\nabla V_{a||})_r^2 \right)$$